

Effects of semidiurnal tidal circulation on the distribution of holo- and meroplankton in a subtropical estuary

HWEY-LIAN HSIEH^{1*}, LAN-FENG FAN^{1,2}, CHANG-PO CHEN^{1,3}, JUUNN-TZONG WU¹ AND WEN-CHENG LIU⁴

¹BIODIVERSITY RESEARCH CENTER, ACADEMIA SINICA, 128 ACADEMIA RD., SEC. 2, NANKANG, TAIPEI 115, TAIWAN, ²INSTITUTE OF OCEANOGRAPHY NATIONAL TAIWAN UNIVERSITY, 1 ROOSEVELT RD., SEC. 4, TAIPEI 106, TAIWAN, ³INSTITUTE OF FISHERIES SCIENCES, NATIONAL TAIWAN UNIVERSITY, 1 ROOSEVELT RD., SEC. 4, TAIPEI 106, TAIWAN AND ⁴DEPARTMENT OF CIVIL AND DISASTER PREVENTION ENGINEERING, NATIONAL UNITED UNIVERSITY, 1 LIENDA, MIAOLI 360, TAIWAN

*CORRESPONDING AUTHOR: zohl@gate.sinica.edu.tw

Received August 21, 2009; accepted in principle February 12, 2010; accepted for publication February 16, 2010

Corresponding editor: Mark J. Gibbons

We examined how tidal changes and which physical factors affected holo- and meroplankton assemblages in a subtropical estuary in Taiwan in February 1999. A factor analysis showed that during tidal flooding, the water mass properties changed from low salinity (5–16) and high particulate organic carbon (POC, 2.6–4.5 mg L⁻¹) content to increasing salinity and high total suspended matter content (29.0–104.5 mg L⁻¹). With a receding tide, the water became more saline again, and its velocity increased (from non-detectable to 0.67 m s⁻¹). One-way ANOVA showed that the distributions of four dominant taxa were affected by the ebb tide and exhibited two distinct groups. The first group consisted of non-motile invertebrate eggs and weakly swimming polychaete sabellid embryos and larvae (at densities of 1.25–1.40 ind. L⁻¹), while the second consisted of better-swimming copepods and polychaete spionid larvae (at densities of 0.70–1.65 ind. L⁻¹). A canonical correlation analysis demonstrated that the former group occurred at sites with greater freshwater input, higher POC content and greater depth, whereas the latter group was significantly associated with sites subject to seawater and faster flows. We propose that a two-layered circulation process and tidally induced oscillations in water movements might account for the distributional differences between these two groups.

KEYWORDS: tidal circulation; holo- and meroplankton distribution; subtropical estuary

INTRODUCTION

Since meroplanktonic larvae function as the supply side of marine benthos, their dispersion plays a key role in replenishing benthic communities (Shanks, 1995). Several studies have documented how meroplanktonic larvae are subject to hydrodynamic constraints under which they act

as passive particles (Shanks *et al.*, 2002, 2003). However, they are also reported to be capable of actively dispersing with flows, particularly those organisms with efficient swimming abilities, such that they can partially counteract hydrodynamic forces (Mariani *et al.*, 2006). Crustacean zoea and megalopa, as well as drifting bivalve post-larvae,

doi:10.1093/plankt/fbq026, available online at www.plankt.oxfordjournals.org. Advance Access publication March 17, 2010

© The Author 2010. Published by Oxford University Press.

This is an Open Access article distributed under the terms of the Creative Commons Attribution Non-Commercial License (<http://creativecommons.org/licenses/by-nc/2.5/uk/>) which permits unrestricted non-commercial use, distribution, and reproduction in any medium, provided the original work is properly cited.

are capable of searching to a greater or lesser degree for suitable currents (Garrison and Morgan, 1999; Queiroga and Blanton, 2004). For example, they perform vertical migrations according to certain tidal phases in order to remain in an estuary (e.g. bivalves, Garrison and Morgan, 1999; zoea and megalopa, Queiroga and Blanton, 2004). Regardless of whether estuarine meroplankton dispersion is active or passive, tidal phase-related factors such as salinity, temperature, chemical substances, current velocity and hydrostatic pressure are reported to be important to their distribution (Garrison and Morgan, 1999; Kingsford *et al.*, 2002).

It has long been suspected that holoplanktonic copepods can migrate vertically and maintain their horizontal position in estuaries by avoiding or utilizing tidal currents of different flow rates and salinities (Wooldridge and Erasmus, 1980). These behavioral responses were proposed for several copepod species as a mechanism that would allow them to remain within estuaries (Wooldridge and Erasmus, 1980). A more recent study showed that under still water conditions, the copepod *Oncaea venusta* performed non-random movements. This implies that copepods can likely direct themselves to avoid or utilize specific corridors in natural systems, although swimming only for a microscopic distance at a time (Seuront *et al.*, 2004). In addition, two-layered circulation, which occurs between lighter surface outflowing and heavier bottom inflowing waters, can account for the successful retention of copepods within estuaries. Such circulation was proposed as aiding the copepods *Acartia longipatella*, *A. natalensis* and *Pseudodiaptomus hessei* to direct their vertical migrations between the two layers in a stratified water column (Wooldridge and Erasmus, 1980; Miller, 1983).

It has been demonstrated in laboratory experiments that some competent polychaete larvae can respond to flow conditions as well as chemical cues during settling (Pawlik *et al.*, 1991). However, these responses are considered insufficient for orientation and navigation in a field water column due to their limited sensory complement and swimming abilities (Kingsford *et al.*, 2002). Pre-competent polychaete larvae are even less well endowed with sensory ability and locomotive devices, so they are thought to be transported like neutrally buoyant particles (Levin, 1986; Kingsford *et al.*, 2002). From the very few available data, the larval distributions of several estuarine polychaete species appear to be correlated with daytime tidal oscillations, while this pattern was not persistent at night (Levin, 1986). These sparse data highlight the need for additional knowledge about the distributions of estuarine non-decapod meroplankton.

The Tanshui River estuary is the largest estuary in northern Taiwan. Here spionid (*Prionospio japonica*, and

several species of *Polydora* and *Pseudopolydora*) and sabellid (*Laonome albicingillum*) larvae dominate the polychaete larval community and occur almost year-round except in summer (June to September) (Hsieh, 1997; Hsieh and Hsu, 1999). The calanoid *Temora turbinata* is among the most dominant holoplanktonic copepods (Yu, 2005). Moreover, a simulation model demonstrated the occurrence and location of a two-layered estuarine circulation in the lower reach of this estuary (Liu *et al.*, 2002). This modeling result and the reported zooplankton locomotive abilities led us to hypothesize that in the Tanshui estuary, the circulation induced by salinity changes during tidal fluctuations may serve as an entrapping force for holoplankton and/or meroplanktonic polychaete larvae. Meanwhile, we also predicted that weaker swimmers act more like passive particles, while stronger swimmers may respond to flow conditions to some extent. In the present study, we simultaneously examined plankton and the physical properties of the water column over a daytime tidal cycle from the flood to the ebb-tide period to determine how the organisms were distributed over the distance from the river mouth to upstream sites and what tidally related factors might be involved in determining their distributions. We focused on: (i) the characteristics of the physical settings of the water masses, (ii) the temporal and spatial distributions of copepod holoplankton and polychaete meroplankton and (iii) the relationships of these distribution patterns with the physical setting of the water mass. The physical setting was determined by examining hydrological and water quality parameters.

METHOD

Study area

The Tanshui River estuarine system, located northwest of Taipei City, is the largest estuary in northern Taiwan (Fig. 1). Upstream areas receive freshwater from the main stream of the Tanshui River and the tributary Keelung River. Semidiurnal tides predominate with an average tidal range of 2.22 m and a spring tidal range of 3.1 m. The water depth in the estuary generally ranges from 2 to >10 m. The deepest locality is near Guandu, where the Tanshui and Keelung Rivers converge.

Saltwater intrudes to ~25 km upstream of the river mouth in both rivers. In addition to the barotropic flows forced by the tides and the river discharge, the hydrological features reveal that baroclinic flow forced by seawater intrusion is another important transport mechanism in this estuarine system (Liu *et al.*, 2002). A salinity profile of the water column indicates that it is

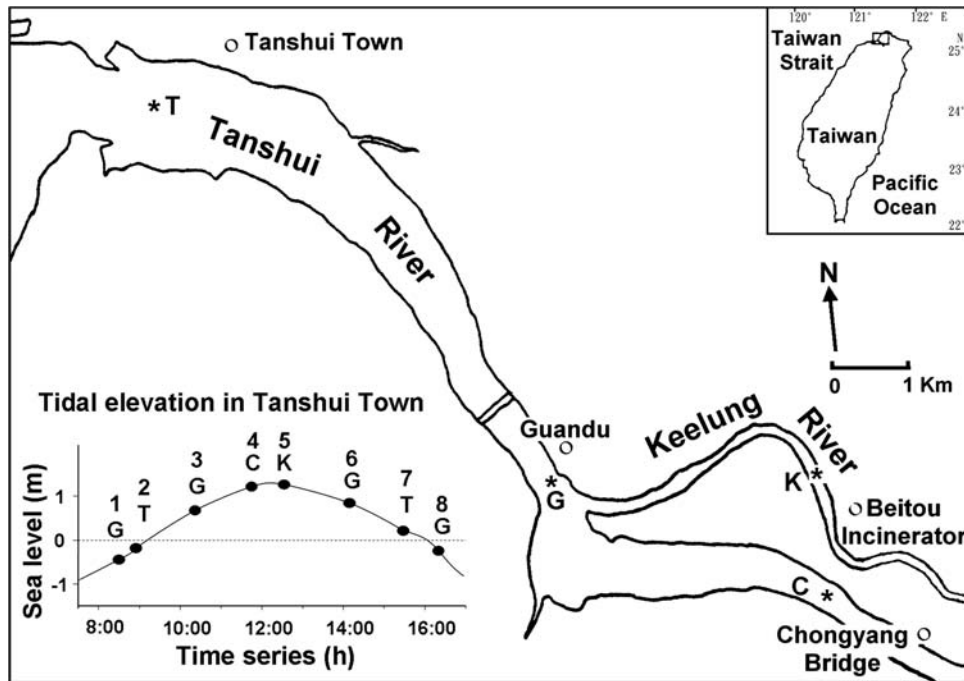


Fig. 1. Study site in the Tanshui River system of northern Taiwan. Relative tidal elevations and the sampling route during the semidiurnal tidal cycle are shown on the bottom left-hand side. The Arabic numerals (1–8) refer to the sampling series. The capital letters T, G, C and K refer to the sites at Tanshui, Guandu, the Chungyang Bridge in the main channel and the Beitou Incinerator in the Keelung River, respectively.

well mixed during the flood-tide period and partially mixed through the ebb tide (Liu *et al.*, 2002).

This circulation regime was also associated with a turbidity maximum observed near the Guandu section where the depth is greatest (approximately 12–14 m, Hsu *et al.*, 2006). Concentrations of suspended particles are comparatively low in both the surface and bottom waters of the midsection (18 km from the river mouth) but increase in the bottom of the Guandu section (8 km from the river mouth) where settling velocities are higher. This gradient implies that suspended particles are advected seaward and deposited further downstream (Liu, 2005).

Sampling sites and sequences

During a semidiurnal tidal period on 2 February 1999, eight sample sets, each with three sampled depths, were collected at four sites in the Tanshui River estuarine system (Fig. 1). For each sampling set, water and plankton were simultaneously collected. The timing coincided with a near-spring tidal phase, so there was a large tidal fluctuation range. The tidal phase near the river mouth (Tanshui City, Fig. 1) reached the highest level at noon (Chinese Naval Hydrographic and Oceanographic Office, 1999). Since the tidal effect on saltwater intrusion is a key factor in this study, all sampling sites

encompassed areas where seawater penetrated. From the river mouth moving upstream, four sites were chosen: the Tanshui site (T) in the lowest reach, the Guandu site (G) where the Keelung River meets the main channel of the Tanshui River and two mid-reach sections below the upper limit of saltwater intrusion, at Chungyang Bridge (C) and at the Beitou Incinerator (K) in the main channel of the Tanshui and Keelung Rivers, respectively.

To compare the differences in water mass characteristics, and holo- and meroplankton distributional characteristics with the tidal phases in both the flood- and ebb-tide periods, we designed a sampling schedule according to the semidiurnal tidal rhythm and applied different sampling frequencies at the four sites. Within the limited daytime sampling period, this sampling scheme allowed us to compare temporal variations occurring in the estuarine region (i.e. sites G and T) in both the flood and ebb phases while also sampling a broad stretch from the river mouth to the upstream sites (i.e. sites C and K). Sampling moved in the direction of the tidal current from commencement of flooding to that of ebbing. Therefore, the water mass at site T was sampled twice, site G four times, and sites C and K once each. The notations of the eight sampling sets are as follows: 1G, 2T, 3G, 4C, 5K, 6G, 7T and 8G (Fig. 1).

Pump sampling, sampling depths and environmental parameters collected

Due to pump avoidance, zooplankton with fast swimming abilities, such as mysids, isopods and amphipods, would be under-sampled compared with those captured using a plankton net (Miller and Judkins, 1981). However, it is difficult to obtain quantitative samples from different depths at the same time using plankton nets. Therefore, we chose a pump sampler and collected slower-swimming zooplankton such as copepods and polychaete larvae.

To ensure that the data reflected the instantaneous characteristics of the water, and holo- and meroplankton assemblages, all fieldwork at each site-time sampling was completed within 5 min. Three sampling depths were discriminated: 0.5 m below the surface (S), mid-water (M) and 1 m above the bottom (B). Each of three submersible pumps (PW-100, with a body diameter of 25 cm, a flow rate of ca. 40 L min⁻¹ and a tube diameter of 1.27 cm) was tied to a rope and dropped to each depth to obtain simultaneous samples. Ten liters of water was pumped for the measurement of environmental parameters, and another four 1.15-L samples of water were taken for plankton collection. Among 19 environmental factors, depth, flow rate, salinity, temperature, pH and conductivity were directly measured in the field. Turbidity; the concentrations of dissolved oxygen (DO), sulfate (SO₄⁻), total nitrogen (TN) and total phosphorus (TP); the contents of total (TSM), small- (SSM), medium- (MSM) and large-sized suspended matter (LSM); the particulate organic carbon (POC) and particulate nitrogen (PN) contents; the chlorophyll (Chl) *a* concentration; and algal abundance were measured in the laboratory after the water samples were brought back to the laboratory in coolers. In the field, plankton samples, each with four replicates, were filtered through an 80- μ m mesh net, and the organisms retained on the mesh were washed into jars, anesthetized with menthol, fixed with 5% formalin and then preserved in 70% ethanol for further analysis. In total, 24 samples (3 depths \times 8 sets of sample site-time), each with 19 environmental factors and one combination of the holo- and meroplankton communities were examined.

Measurement of environmental parameters

The flow rate was measured using an electronic flow meter (no. 1726, San-Ei Electronic Industries, Nagano, Japan). Conductivity was determined using a multiparameter monitoring system (YSI 85, YSI, Yellow Spring, OH, USA). Turbidity was measured using a turbidometer (Orbeco-Hellige, Farmingdale, NY, USA). TSM

was determined using a laser diffraction particle size analyzer (model 715, CILAS US, Madison, WI, USA). This was further separated into particle size fractions of SSM of <40 μ m, MSM of 40–80 μ m and LSM of >80 μ m.

The DO was determined by azide modification of the Winkler method (American Public Health Association, 1992). Briefly, MnSO₄ was added to alkalinized samples, followed by the addition of a potassium iodide/azide-saturated starch solution and titration with sodium thiosulfate. The concentration of sulfate was determined using a sulfate test kit (Merck, Darmstadt, Germany). TN was measured by reducing all of the nitrogenous compounds to ammonium using the Kjeldahl method and then using an ammonium test kit (Merck). To determine TP, water samples were subjected to acid hydrolysis at boiling temperature to convert all of the phosphorus compounds to orthophosphate, and then TP was determined using the ascorbic acid method (American Public Health Association, 1992).

For the analysis of the POC and PN contents, 0.7 L of water was initially passed through a 40- μ m mesh screen, and the particulates retained on pre-combusted glass fiber filters (GF/Fs) were cryo-dried, acidified with 1 N HCl and measured using a CHN analyzer (Perkin Elmer EA 2400 Series II, Waltham, MA, USA).

To determine the Chl *a* concentration in water, the particulates retained on the GF/Fs after filtration under reduced pressure were extracted with methanol (100%) at 60°C for 30 min in the dark. Then the supernatant after centrifugation (3000 \times g for 10 min) was examined using a spectrophotometer, and the concentration of Chl *a* was calculated following the description of the APHA (APHA, 1992).

Samples for measuring algal abundance were collected with a plankton net with a mesh size of 10 μ m, fixed in Lugol's iodine solution immediately after collection, and stained with a Coomassie brilliant blue solution (1 g dissolved in 100 mL of 95% ethanol) at room temperature. After being washed with deionized water, samples were filtered onto cellulose nitrate membrane filters (with a pore size of 0.45 μ m, Sartorius, Germany) and mounted on a slide with immersion oil after the membrane filters had been completely dried. Algal cells were then counted under a phase contrast microscope (Wu, 1999).

Measurements of zooplankton samples

The term zooplankton used here indicates a mixture of holoplankton copepods and meroplankton, including planktonic eggs, embryos and developing larvae of

benthic invertebrates. Most of the zooplankton were only identified to higher taxonomic levels such as phylum or order, except for polychaetes, which were further identified to species. Since calanoid copepods comprised 61% of the species and 70% of the abundance of the copepod assemblage in the Tanshui estuary (Yu, 2005), the calanoids were the most dominant component of the copepod taxon. Some of the zooplankton were classified as collective groups such as “invertebrate eggs” and “trochophore larvae”. Herein, invertebrate eggs consisted of eggs from non-polychaete taxa. Trochophore larvae also excluded polychaete trochophores. Three polychaete species were found. One was the sabellid, *Laonome albicigillum*; the other two were the spionids, *Prionospio japonica* and, presumed to be, *Malacoceros indicus* (Hsieh, 1995a, 1997). Sabellid planktonic offspring were at various development stages, including eggs, embryos, trochophores and segmented larvae, which comprised 3.9, 37.0, 24.4, and 34.7%, respectively, of the total sabellid offspring abundance. We used the term “sabellid embryos and larvae” to accommodate all of the above-mentioned stages. We were not able to specifically identify spionid larvae for our study estuary, but the morphology of one spionid larval group resembled that of *M. indicus*; thus, we tentatively used *M. indicus* to indicate this larval group (communication with Vasily I. Radashevsky, Institute of Marine Biology, Russian Academy of Science, Vladivostok, Russia). The term “spionid larvae” represented larvae combined from both spionid species in which *M. indicus* comprised 93% of the total spionid larval abundance. The number of individuals in each taxon was counted using a dissecting microscope. The abundance of each taxon was expressed as the mean number of individuals per liter.

Statistical analysis

To determine the most important factors, we conducted a factor analysis on the 19 parameters using the principal component method (Rencher, 1995). Ordination of the 24 water samples was subsequently carried out to identify the characteristics of the physical settings of these water masses.

In order to overcome the uncertainty of distributional normality due to the small sample size of our biological data, nonparametric statistics were performed for a univariate analysis of variance (ANOVA). We compared the densities of each of the dominant taxa that comprised more than 80% of the total abundance of the entire holo- and meroplankton community using a nonparametric ANOVA with the Kruskal–Wallis test (Hollander and Wolfe, 1999) to see whether there were

distributional differences among sample settings. Four settings were examined: (i) three depths, (ii) four tidal phases at the Guandu site, (iii) the influences of flood tides from the estuary to the upstream reaches and (iv) the influences of ebb tides from the upstream sections to the river mouth. When significant ANOVA results were found, we performed a multiple-means comparison using Dunn’s test (Hollander and Wolfe, 1999). Moreover, to interpret the relationships between the dominant holo- and meroplankton taxa and environmental factors, a canonical correlation analysis was performed (Digby and Kempton, 1987). For the multivariate factor analysis and canonical correlation analysis, the data distributions were consistent with the assumption of normality (Peterson and Stromberg, 1998). All significance levels were 0.05 except for the second canonical variable of the canonical correlation analysis and for the Dunn’s test, which were 0.1 (Cavadias *et al.*, 2001) and 0.25 (Gibbons, 1985), respectively. All statistical analyses were conducted using the software package SAS 9.1 (SAS Institute, 2003).

RESULTS

Environmental measurements and characterization of the water masses

Nineteen environmental factors for the water recorded at four sites and three depths throughout the studied tidal rhythm are shown in Table I. Using a factor analysis, the most important environmental elements of the water masses were identified. The first two principal factors together explained nearly 65% of the total variation, with each explaining 43 and 21.3%, respectively. On axis factor 1, salinity, pH, conductivity and DO were positively correlated with the axis, while the POC and PN contents, and TN and TP concentrations were negatively correlated with the axis (each with factor loading values of >0.75, Fig. 2). The former group reflects seawater-associated characteristics, whereas the latter represents freshwater-influenced organic matter enrichment. In order to avoid redundancy when classifying the characteristics of the water masses, we abstracted the most important elements, salinity and POC content, from the two groups on the factor 1 ordination (with factor loadings of 0.98 and -0.92 , respectively). On axis factor 2, the TSM, SSM and MSM contents, and turbidity were highly positively correlated with the axis (Fig. 2). Among these, we chose TSM content as the most important element for representing flow-velocity-driven particle transport (with a factor loading of 0.93).

Table I: Measures of water environmental parameters at four sites during the sampling sequence

Sampling sequence	Time	Site	Layer	Depth (m)	Flow rate (m/s)	Salinity	Temp. (°C)	Cond.			DO (mg L ⁻¹)	TSM (mg L ⁻¹)	SSM (mg L ⁻¹)	MSM (mg L ⁻¹)	LSM (mg L ⁻¹)	POC (mg L ⁻¹)	PON (mg L ⁻¹)	Sulfate (mg L ⁻¹)	TN ^a (mg L ⁻¹)	TP ^a		
								pH	(ms cm ⁻¹)	Turb. (NTU)										(μg L ⁻¹)	(μg L ⁻¹)	(μg L ⁻¹)
1	08:30	G	S	0.50	-0.45	5	17.4	7.0	3.3	17.7	1.2	13.0	10.9	0.5	1.6	4.5	0.69	185	8.9	89.2	1.5	6240
			M	5.25	0.00	14	17.2	7.3	15.6	20.2	1.6	25.0	18.8	3.8	2.5	2.9	0.48	826			1.0	1930
			B	9.50	0.00	16	18.2	7.3	18.4	21.4	1.6	31.0	29.1	1.9	0.0	2.6	0.34	936			1.1	2700
2	08:55	T	S	0.50	-0.40	25	17.8	7.6	16.2	17.1	2.9	28.0	16.5	0.6	10.9	1.1	0.14	1127	3.6	54.7	0.8	7590
			M	2.20	0.00	25	18.1	7.6	23.4	21.0	3.3	36.5	29.2	5.9	1.4	1.2	0.14	1161			0.6	7920
			B	3.40	0.00	25	18.0	7.6	27.3	23.8	3.7	63.5	53.2	9.5	0.8	1.4	0.16	1171			0.7	7410
3	10:22	G	S	0.50	-0.37	22	20.3	7.4	23.4	21.8	1.6	29.0	17.8	9.4	1.8	0.9	0.12	1072	4.4	66.8	0.7	8710
			M	5.25	0.00	22	20.3	7.4	24.4	26.6	2.7	54.5	45.0	8.9	0.7	1.7	0.20	706			1.1	6350
			B	9.50	0.00	22	19.9	7.4	24.4	49.8	2.7	104.5	71.8	17.0	15.7	2.2	0.28	702			1.6	10400
4	11:45	C	S	0.50	-0.43	15	22.7	7.4	18.4	9.0	3.5	19.5	17.8	0.5	1.2	2.0	0.26	581	5.2	94.3	1.6	18750
			M	5.10	0.00	18	22.4	7.3	21.5	19.6	1.9	27.0	24.0	2.0	1.0	1.6	0.20	649			1.1	16060
			B	9.20	0.00	18	22.2	7.3	21.5	38.6	1.9	38.5	34.2	4.3	0.0	1.9	0.21	649			1.2	15350
5	12:33	K	S	0.50	-0.30	20	21.4	7.3	20.5	14.1	2.0	26.0	24.4	1.3	0.3	1.1	0.11	675	4.2	32.4	0.8	11780
			M	1.75	0.00	20	21.5	7.4	21.5	26.7	2.4	28.5	20.3	2.8	5.4	1.1	0.13	691			0.9	15160
			B	2.50	0.00	20	21.4	7.4	22.5	34.3	1.8	20.0	18.5	0.3	1.2	1.3	0.11	697			0.9	12750
6	14:09	G	S	0.50	0.43	22	21.2	7.6	23.4	6.0	3.8	20.0	18.0	0.0	2.0	0.8	0.07	702	4.0	34.8	0.9	10950
			M	7.00	0.24	35	20.7	8.1	33.2	20.8	7.4	28.5	13.5	1.4	13.5	0.6	0.04	846			1.1	3260
			B	13.00	0.00	35	20.6	8.2	29.3	21.4	7.5	34.5	11.2	0.0	23.3	0.6	0.04	861			1.2	2450
7	15:28	T	S	0.50	0.54	28	20.0	7.9	27.3	8.8	6.0	25.0	24.8	0.3	0.0	0.8	0.07	765	2.7	23.7	0.6	6800
			M	2.75	0.31	35	20.1	8.2	31.2	16.0	6.9	28.0	16.8	0.0	11.2	0.5	0.04	838			1.0	3120
			B	4.50	0.00	35	20.0	8.2	29.3	23.2	7.3	29.0	10.2	1.5	17.4	0.6	0.04	849			1.1	2850
8	16:20	G	S	0.50	0.67	18	21.1	7.4	19.5	6.2	1.9	11.0	7.2	1.2	2.6	1.6	0.22	654	5.2	77.1	0.9	9440
			M	7.00	0.41	21	21.4	7.4	23.4	15.3	3.0	14.0	13.3	0.0	0.7	1.3	0.15	691			1.0	12410
			B	13.00	0.00	33	20.8	8.0	31.2	18.4	6.2	29.0	17.8	1.5	9.8	0.6	0.06	830			0.7	790

The abbreviations of environmental parameters are described in Method except the following: Algae, algal abundance; Chl *a*, chlorophyll *a* concentration; Cond., conductivity; Temp., temperature.

^aValues of three layers mixing; a negative “-” value for the flow rate indicates an upstream flow direction, and 0.00 indicates that the flow rate was too slow to measure.

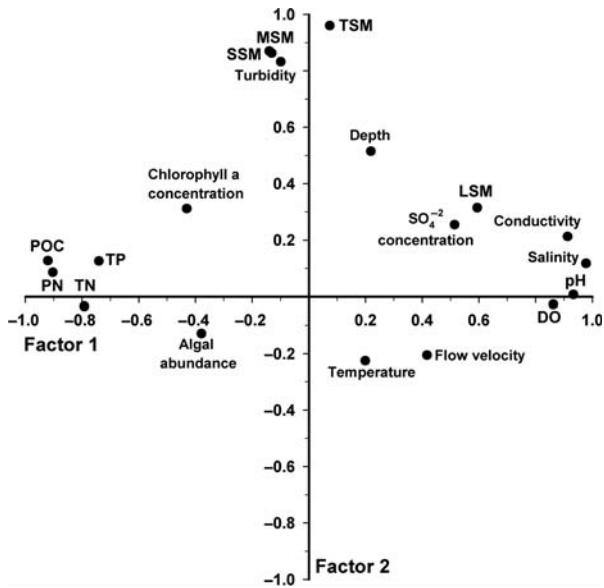


Fig. 2. Ordinations of 19 environmental parameters by the factors 1 and 2 using a factor analysis. The abbreviations of the parameters are given in "Method".

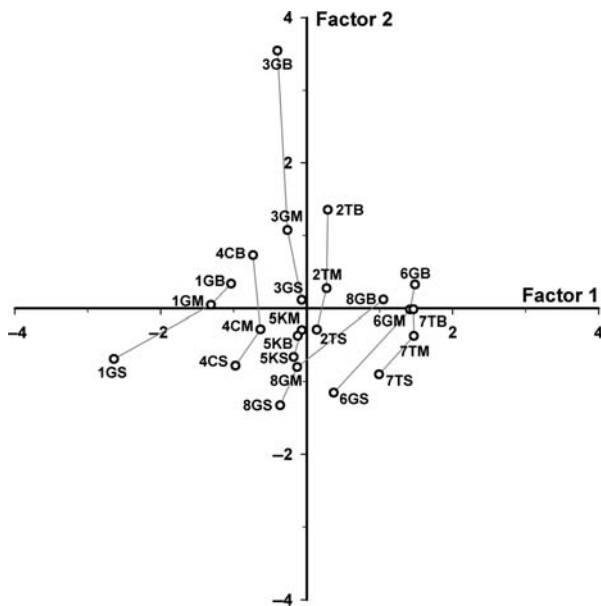


Fig. 3. Ordinations of 24 water samples by the factors 1 and 2. The Arabic numerals (1–8) refer to the sampling series. The capital letters S, M and B refer to the surface, middle and bottom depths, respectively.

When all samples were ordinated by axis factors 1 and 2, the effect of sampling depth was clear (Fig. 3). The water's physical and biotic characteristics (Chl *a* concentration and algal abundance) could be aligned in a nearly parallel fashion between the depths from the surface to the bottom, and the gradients of salinity, and

POC and TSM contents except those at site 5K (Figs 2 and 3). At the Guandu and Tanshui estuarine sites, the water column was first overridden by freshwater and contained a high POC content during the early flooding period (samples 1GS, 1GM and 1GB; Figs 2 and 3). Subsequently, as the tide continued to come in, the water column became saline and contained less POC (samples 2TS, 2TM and 2TB). This trend was particularly conspicuous during the ebb period at Tanshui (samples 7TS, 7TM and 7TB) and in the subsurface layers at Guandu (samples 6GM, 6GB and 8GB). Finally, in the late ebb period, the surface and mid-water at Guandu were again dominated by freshwater (samples 8GS and 8GM). When flooding was prevalent and approaching the high-slack tide, the tide washed further upstream where the water column in the Tanshui River at the Chungyang Bridge (samples 4CS, 4CM and 4CB) was less saline but had more POC content than that in the Keelung River at the Beitou Incinerator (samples 5KS, 5KM and 5KB).

Generally, during flooding, the TSM content of the water in the subsurface layers, especially in the bottom layers, increased and reached the highest level at 3GB (Fig. 3). Later, the water TSM content began to decrease when flooding approached high tide, and it became much diminished after the tide receded.

Distributions of zooplankton assemblages

The densities of the entire zooplankton assemblages averaged $7.5 \pm 0.6 \text{ ind. L}^{-1}$ during the course of sampling. Zooplankton consisted of 16 identifiable taxa. Their relative abundances showed that the four most abundant taxa accounted for more than 80% of the total abundance of the zooplankton (Table II). These four taxa were polychaete spionid larvae (*Malacoceros indicus* and *Prionospio japonica* combined, 27.0%), the invertebrate egg group (23.0%), the polychaete sabellid *Laonome albicingillum* (embryos and larvae combined, 20.5%) and the copepods (11.4%).

The four dominant taxa exhibited spatial and temporal distribution patterns distinct from one another (Figs 4–6 and Table III). Regarding depth distribution, these taxa exhibited no depth gradients, except for the sabellids. Sabellid embryos and larvae had a weak depth tendency ($P < 0.05$, Table III), having a higher density in subsurface layers than in the surface layer.

Examining their concurrence with the tidal rhythm at the Guandu site in particular, both the spionid and sabellid densities changed with the tidal setting, but the trends differed from each other ($P < 0.01$ for spionids, $P < 0.001$ for sabellids, Table III, Fig. 4). The spionids had a relatively higher density in the early receding tide

Table II: Density (mean ± SE) of zooplankton and meroplankton assemblages and their relative and cumulative percents

Zooplankton assemblage	Density (ind. L ⁻¹ , n = 96)	Relative percent (%)	Cumulative percent (%)
Spionid larvae (<i>Malacoceros indicus</i> ^a and <i>Prionospio japonica</i> pooled)	1.65 ± 0.40	27.00	27.0
Invertebrate eggs (excluding polychaetes)	1.40 ± 0.19	23.00	50.1
Sabellid embryos and larvae pooled (<i>Laonome albicingillum</i>)	1.25 ± 0.19	20.50	70.6
Copepods (mostly Calanoids)	0.70 ± 0.13	11.40	82.0
Copepod nauplii	0.40 ± 0.06	6.54	88.6
Trochophore larvae (excluding polychaetes)	0.32 ± 0.08	5.20	93.8
Nematodes	0.21 ± 0.05	3.42	97.2
Bivalve larvae (advanced stage)	0.04 ± 0.02	0.59	97.8
Chaetognaths	0.04 ± 0.02	0.59	98.4
Cnidarians	0.03 ± 0.02	0.45	98.8
Veliger larvae (bivalves and gastropods)	0.02 ± 0.01	0.30	99.1
Amphipods	0.02 ± 0.02	0.30	99.4
Barnacle nauplii	0.01 ± 0.01	0.15	99.6
Flatworms	0.01 ± 0.01	0.15	99.7
Flatworm larvae	0.01 ± 0.01	0.15	99.9
Insects	0.01 ± 0.01	0.15	100.00

Taxa are listed in descending order of density.

^aSee Method for species identification.

than in the early flood tide (6G 6.88 ± 2.55 versus 1G 0.22 ± 0.11 ind. L⁻¹). Conversely, the sabellids were less abundant in the early receding tide relative to the late receding tide and in the early flood tide (6G 0.15 ± 0.15 versus 8G 2.46 ± 0.51 and 1G 3.04 ± 0.94 ind. L⁻¹).

With respect to the spatial distributions of the four dominant taxa during the flood-tide period, only the sabellids showed significant variation with locality and time as the flood progressed ($P < 0.05$, Table III, Fig. 5). The sabellid density appeared to be greater in the lower reach of the Tanshui River in the initial flooding period and in the upstream area of the main river channel at high-slack tide than in the estuarine site (1G 3.04 ± 0.94 and 4C 2.10 ± 0.56 versus 2T 0.51 ± 0.29 ind. L⁻¹).

Comparing the distributions during the ebb-tide period, all four taxa displayed significant density changes with locality and time, and with one another (Fig. 6). The spionid larval densities were markedly

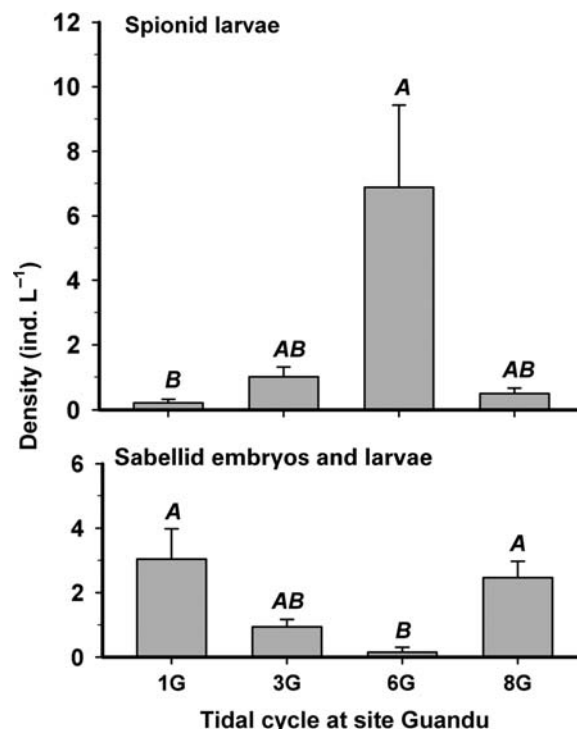


Fig. 4. Density changes (mean ± SE) of spionid larvae, and sabellid embryos and larvae during the study tidal cycle at the Guandu site. Densities with the same italicized letters do not significantly differ using Dunn's test.

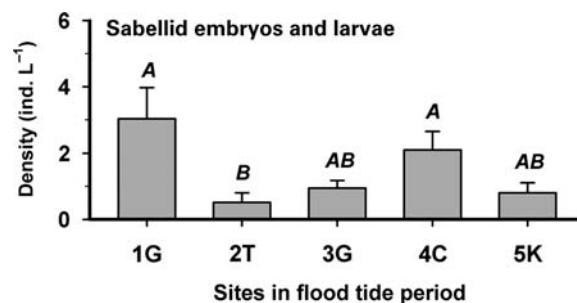


Fig. 5. Density changes (mean ± SE) of sabellid embryos and larvae from the estuary to upstream reaches during the flood-tide period. Densities with the same italicized letters do not significantly differ using Dunn's test.

higher in the estuarine area when the tide had retreated about halfway than in the upstream area of the main river channel at high-slack tide when the tide began to recede ($P < 0.01$, Table III; 6G 6.88 ± 2.55 and 7T 3.48 ± 0.93 versus 4C 0.22 ± 0.11 ind. L⁻¹, Fig. 6). Similar to spionid larvae, copepods also exhibited a spatial-temporal gradient with a greater density present at the estuarine site when the tide had receded halfway than at the upstream site when the tide began to fall ($P < 0.01$, Table III; 7T 2.46 ± 0.79 and 0.80 ± 0.23

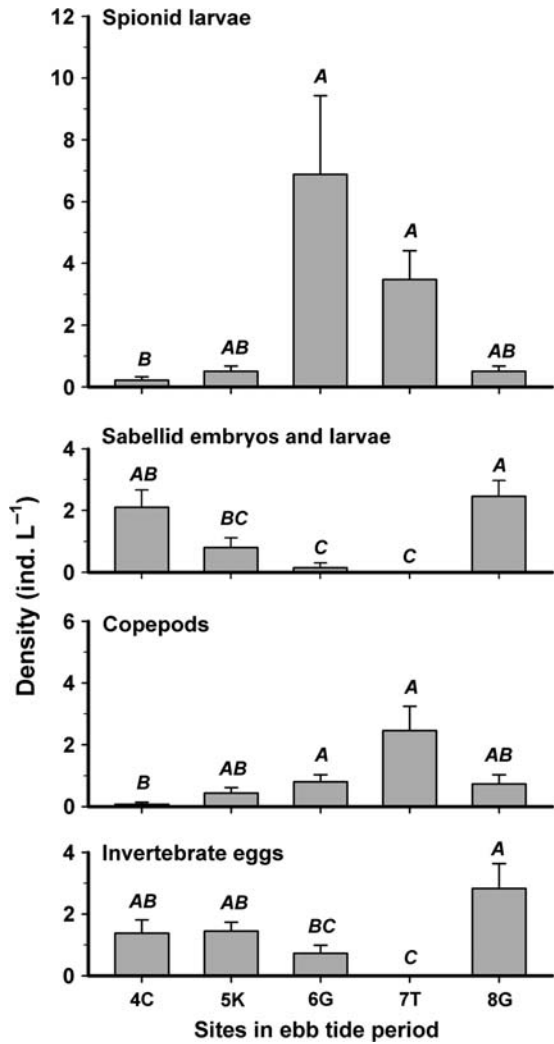


Fig. 6. Density changes (mean ± SE) of spionid larvae, sabellid embryos and larvae, copepods and invertebrate eggs from upstream reaches to the river mouth during the ebb-tide period. Densities with the same italicized letters do not significantly differ using Dunn’s test.

versus 4C $0.07 \pm 0.07 \text{ ind. L}^{-1}$, Fig. 6). In contrast, sabellid embryos and larvae showed a reverse gradient. There appeared to be fewer in the estuarine area when the tide had retreated halfway than at the upstream site when the tide began to fall, and they subsequently gathered at the Guandu site when the tide approached the low-slack phase ($P < 0.001$, Table III; 6G 0.15 ± 0.15 and 7T none versus 4C 2.10 ± 0.56 and 8G $2.46 \pm 0.51 \text{ ind. L}^{-1}$, Fig. 6). Moreover, the invertebrate eggs had a distributional trend comparable with that of the sabellids. There were rather few invertebrate eggs at the estuarine site, but they were abundant at Guandu and the two upstream sites ($P < 0.001$, Table III; 8G 2.83 ± 0.80 , 5K 1.45 ± 0.29 and 4C 1.38 ± 0.43 versus 7T none ind. L^{-1} , Fig. 6).

Table III: Spatial and temporal distinctions for the dominant zooplankton and meroplankton assemblages analyzed using Kruskal–Wallis ANOVA test

Assemblage	Grouping	df	χ^2 value	P-value
Spionid larvae	Sampling depth	2	1.18	ns
	Tidal cycle at Guandu	3	11.26	**
	Sites in flood-tide period	4	7.23	ns
	Sites in ebb-tide period	4	16.39	***
Sabellid embryos and larvae	Sampling depth	2	6.10	*
	Tidal cycle at Guandu	3	17.24	***
	Sites in flood-tide period	4	11.49	*
	Sites in ebb-tide period	4	33.86	***
Copepods	Sampling depth	2	0.59	ns
	Tidal cycle at Guandu	3	6.54	ns
	Sites in flood-tide period	4	6.35	ns
	Sites in ebb-tide period	4	15.19	**
Invertebrate eggs	Sampling depth	2	5.25	ns
	Tidal cycle at Guandu	3	6.16	ns
	Sites in flood-tide period	4	2.33	ns
	Sites in ebb-tide period	4	21.96	***

ns, no significant difference.
 * $0.01 < P < 0.05$.
 ** $0.001 < P < 0.01$.
 *** $P < 0.001$.

Relationships of zooplankton distributions with environmental parameters

The first two canonical correlations between the four dominant taxa and four environmental parameters were both significant, and explained 60.0 and 25.1% of the total variance, respectively ($r_1 = 0.71$, approx. $F_{(16,50)} = 2.56$, $P = 0.01$; $r_2 = 0.54$, approx. $F_{(9, 42)} = 1.98$, $P = 0.07$; Fig. 7). In the first canonical variable, the densities of sabellid embryos and larvae, and invertebrate eggs were positively correlated with the water depth and POC content but negatively correlated with salinity. In the second canonical variable, the densities of copepods and spionid larvae were positively correlated with salinity and flow velocity but negatively correlated with the POC content (Fig. 7).

DISCUSSION

In this study, we used a sampling technique that enabled a daytime collection programme intimately linked with tidal flows throughout a semidiurnal tidal rhythm in the Tanshui River estuarine system. Our results clearly demonstrated a daytime scenario in which the spatial and temporal dispersions of polychaete spionid larvae, sabellid embryos and larvae, copepods and invertebrate eggs were affected by the tidal phase, during which the ebb rhythm rather than the flood rhythm was more important. The associations of these organisms varied with water masses that were

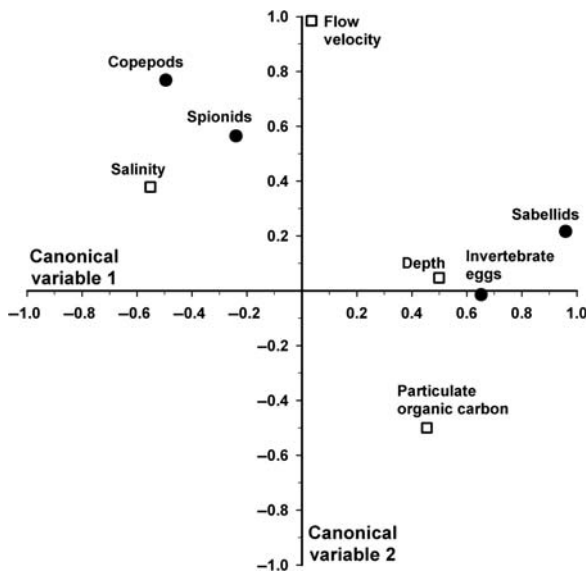


Fig. 7. Ordinations and relationships among the four taxa (spionid larvae, sabellid embryos and larvae, copepods and invertebrate eggs) and four environmental parameters (depth, flow velocity, particulate organic carbon content and salinity) by the first two canonical variables using a canonical correlation analysis.

distinct in salinity, depth, POC content and flow velocity. Comparatively, spionid larvae seemed to display a slightly more active component of dispersion than the neutral buoyant capability used by sabellids for dispersal.

Relative locomotory capabilities of holo- and meroplankton taxa

The four dominant taxa in the present study appeared to be distinguishable as two groups that differed in their abilities to respond to water masses for dispersion (Figs 6 and 7). One group consisted of embryos and larvae of the sabellid *Laonome albicigillum*, as well as invertebrate eggs, while the other comprised two spionid species, *Malacoceros indicus* and *Prionospio japonica*, and copepods. Invertebrate eggs and sabellid embryos are at a stage where they have not yet developed any locomotive cilia; thus, they are immotile. In addition, sabellid larvae are lecithotrophic and develop rapidly, and their settlement is completed within 26–33 h after fertilization; they thus have low dispersal ability (Hsieh, 1995a, b, 1997).

Comparatively, spionids and copepods appeared to possess greater locomotive ability. Copepods are known to be capable of non-random movements in still water conditions, which have been suggested to be an efficient strategy in terms of foraging success, barrier avoidance or utilization of microscale patches (Seuront *et al.*,

2004). The spionid larvae of *Malacoceros indicus* and *Prionospio japonica* found in this study had reached the segmented stages; at this point, they possess several sets of ciliary bands, including the prototroch, gastrotroch, nototroch and telotroch, which function in swimming (Pernet *et al.*, 2002). Moreover, spionid larvae are larger than sabellid larvae; thus, spionid larvae have relatively more muscle. Both the ciliation and muscles of spionid larvae appear to be better suited for swimming than those of the sabellid *Laonome albicigillum* (Pernet *et al.*, 2002; H. L. Hsieh, unpublished results). Based on the dissimilar functional morphologies, we think that the discrepancy in locomotory utility distinguishes the two groups in terms of dispersion mechanisms involving biological components.

Relations of sabellid embryos and larvae, and invertebrate egg group distributions with the physical properties of the water masses

The distributional trends of the two groups characterized in this study differed along the physical gradients of the water masses (Figs 2, 3 and 7). Sabellid embryos and larvae, and invertebrate eggs tended to spread to the upper river reaches and deeper localities where the water mass was dominated by freshwater as seen in the 4C and 1G settings. These waters were characterized not only by lower salinities (5–20), but also by greater POC contents (1.6–4.5 mg L⁻¹) and greater depths (9.2–9.5 m, see Table III). The fact that their occurrence increased with the POC content may reveal a companion effect associated with the physical properties of freshwater. This phenomenon was less related to a biologically active response because the freshwater conveying them happened to be POC enriched, and the sabellid larvae were yolk laden and thus non-feeding.

At the Guandu site, the bimodal abundance distribution exhibited by sabellid embryos and larvae throughout a tidal cycle (Fig. 4) was similar to that reported in several other spionid species and a bivalve species in Mission Bay, California (Levin, 1986). Levin suggested that tidal oscillations were attributable to this bimodal distribution. Considering the inability of sabellid embryos and larvae to propel themselves through water, tidally induced advective transport may contribute profoundly to the formation of this type of abundance oscillation. The early flood tide initiated the first peak as it carried a dense batch of sabellids by the Guandu site, whereas the early ebb tide on its return course created the second peak (1G and 8G samples, Figs 1 and 4). We ruled out the possibility that these peaks were due to synchronization of spawning because

the sabellid *Laonome albicingillum* is not a synchronous reproducer (Hsieh, 1995a).

The tendency for sabellid embryos and larvae to be distributed in the subsurface layers might be attributed to their spawning mode and lecithotrophic development. Hsieh (Hsieh, 1995a) observed that their eggs are released into ambient water in mucous strings. The mucous string holds the developing embryos together until the mucus gradually disintegrates or until the trochophore larvae have gained motility. In addition, the entire larval development relies on the laden yolk. These features imply that the mucus and yolk probably serve as a drag on the embryos or larvae, thus retaining them in deeper water rather than allowing them to float to the surface.

Relationships of spionid larval and copepod distributions with the physical properties of the water mass

Copepods and spionid larvae were distributed in the lower estuarine area where the water mass was dominated by seawater with higher flow velocities but lower POC contents, as reflected in the 6G (the Guandu site) and 7T (the Tanshui site) settings (Figs 6 and 7, Table III). This single-mode distribution cannot be explained by the tidal oscillation process since their abundances did not change in association with the tidal rhythm. Spionid larvae exhibit positive phototaxis, whereas copepods show various levels of phototaxis dependent on the species and diel migration mode (e.g. Levin, 1986; Chae and Nishida, 2004), and reveal active responses to environmental cues. However, unlike crab larvae, whose vertical and lateral migration ability in estuaries is well documented, copepods and spionid larvae are not known to be capable of adjusting themselves toward gradients of salinity or POC content on a large scale in the field (Wooldridge and Erasmus, 1980; Kingsford et al., 2002). The presence of correlations between copepod and spionid larval densities, and decreasing POC content or increasing flow velocity do not imply that these organisms can select for or against these gradients. Rather, such correlations are a concomitant event with the nature of seawater-dominated ebb-tide water.

The larval abundance of several spionid species, such as *Pseudopolydora paucibranchiata*, *Polydora ligni* and *Rhynchospio arenicola*, reached its peak when tidal current velocities were greatest (Levin, 1986). Increased current velocity was reported to induce active swimming in brachyuran crab larvae (Sulkin, 1984), and increased flow and salinity were proposed as stimulating upward swimming in bivalve larvae (Miller, 1983). Nevertheless,

passive aggregation by lee eddies was considered the most likely transport method of spionid larvae (Levin, 1986). Passive dispersion by the back and forth movement of water with upwelling and downwelling events across a shelf was also documented for some bivalve and polychaete larvae that use cilia for propulsion (Shanks et al., 2002, 2003). In the estuary studied here, previous investigations showed that suspended particles were concentrated near the Guandu site, especially under the low river discharge in the Tanshui River (Hsu et al., 2006). Two mechanisms involving local deep-channel bathymetry and two-layered estuarine circulation can evidently account for the suspension entrapment here because the resultant flow was almost negligible. It was further suggested that a long-term trapping capacity, although weak, is present in the lower part of the Tanshui River estuary (Hsu et al., 2006). Taking the ambient physical entrapment forces together with these organisms' limited swimming abilities, we believe that the aggregation of copepods and spionid larvae in and below the Guandu area can be predicted by hydrodynamic processes that are mainly controlled by interactions of bathymetry and estuarine two-layered tidal circulation.

The limited swimming ability does not mean that the spionid larval *Malacoceros indicus* and *Prionospio japonica* cannot disperse widely. In fact, they were found at the upstream sites 4C and 5K, although in small numbers. It was often observed that many spionid larvae swim rapidly toward the water surface when released into ambient water (Fetzer, 2003). Some bivalve larvae, known as slow-swimming larvae, appear to be capable of overcoming certain flow fields, thus maintaining a nearshore distribution (Shanks et al., 2003). These findings suggest that we cannot rule out the possibility that spionid larvae may be able to escape the limits imposed by current or salinity gradients, particularly under a stationary flow regime at the time when the two-layered circulation is prevalent. As a result, spionid larvae can perform vertical movement and subsequently take advantage of strong surface currents for an upstream dispersion. A previous study also recorded few adults of *P. japonica* from reaches above 5K with sediment salinities of <2 in spite of the majority being primarily distributed in the lower estuary where sediment salinities ranged from 15 to 30 (Hsieh, 1995a, b; HL Hsieh, unpublished results). *Malacoceros indicus* and members of the genus *Prionospio* are regarded as having the potential for moderate- to long-distance dispersal (Hsieh, 1994; Carson and Hentschel, 2006). This wide dispersion may be attributed in part to the aforementioned biologically active component, swimming ability.

ACKNOWLEDGEMENTS

We sincerely thank Dr D. Sheehy, Aquabio Inc., Arlington, MA, USA; and Mr D. Chamberlin, Taipei, Taiwan, for reading the manuscript. The authors are very grateful to the anonymous reviewers for their constructive comments. We also thank Mr. Re-Bin Chen for assisting with data collection and Dr Shou-Chung Huang for discussions. This study complies with the current laws of the country in which it was performed.

FUNDING

This study was funded through Thematic Research Program by Academia Sinica, Taiwan.

REFERENCES

- American Public Health Association (APHA), American Water Works Association and Water Pollution Control Federation. (1992) *Standard Methods for the Examination of Water and Wastewater*, 18th edn. APHA, Washington, DC.
- Cavadias, G. S., Ouarda, T. B. M. J., Bobee, B. *et al.* (2001) A canonical correlation approach to the determination of homogeneous regions for regional flood estimation of ungauged basins. *Hydrol. Sci. J.*, **46**, 499–512.
- Chae, J. and Nishida, S. (2004) Swimming behaviour and photore-sponses of the iridescent copepods, *Sapphirina gastrica* and *Sapphirina opalina* (Copepoda: Poecilostomatoida). *J. Mar. Biol. Assoc. UK*, **84**, 727–731.
- Carson, H. S. and Hentschel, B. T. (2006) Estimating the dispersal potential of polychaete species in the Southern California Bight: implications for designing marine reserves. *Mar. Ecol. Prog. Ser.*, **316**, 105–113.
- Chinese Naval Hydrographic and Oceanographic Office. (1999) *Tide table*. Combined Logistics Command, Ministry of National Defense, Taipei, Taiwan, (in Chinese).
- Digby, P. G. N. and Kempton, R. A. (1987) *Multivariate Analysis of Ecological Communities*. Chapman and Hall, London, 216 pp.
- Fetzer, I. (2003) Distribution of meroplankton in the southern Kara Sea in relation to local hydrographic pattern. *Proc. Mar. Sci.*, **6**, 195–212.
- Gibbons, J. D. (1985) *Nonparametric Methods for Quantitative Analysis*, 2nd edn. American Sciences Press, Columbus, OH, pp. 157–204.
- Garrison, L. P. and Morgan, J. A. (1999) Abundance and vertical distribution of drifting, post-larval *Macoma* spp. (Bivalvia: Tellinidae) in the York River, VA, USA. *Mar. Ecol. Prog. Ser.*, **182**, 175–185.
- Hollander, M. and Wolfe, D. A. (1999) *Nonparametric Statistical Methods*, 2nd edn. J. Wiley, NY, 787 pp.
- Hsieh, H. L. (1994) Larval development and substrate preference at settlement in *Pseudopolydora diopatra* (Polychaeta: Spionidae). *Invertebr. Reprod. Dev.*, **25**, 205–214.
- Hsieh, H. L. (1995a) *Laonome albicingillum*, a new fan worm species (Polychaeta: Sabellidae: Sabellinae) from Taiwan. *Proc. Biol. Soc. Wash.*, **108**, 130–135.
- Hsieh, H. L. (1995b) Spatial and temporal patterns of polychaete communities in a subtropical mangrove swamp—influences of sediment and microhabitat. *Mar. Ecol. Prog. Ser.*, **127**, 157–167.
- Hsieh, H. L. (1997) Self-fertilization: a potential fertilization mode in an estuarine sabellid polychaete. *Mar. Ecol. Prog. Ser.*, **147**, 143–148.
- Hsieh, H.-L. and Hsu, F. (1999) Differential recruitment of annelids onto tidal elevations in an estuarine mud flat. *Mar. Ecol. Prog. Ser.*, **177**, 93–102.
- Hsu, M. H., Wu, C. R., Liu, W. C. *et al.* (2006) Investigation of turbidity maximum in a mesotidal estuary, Taiwan. *J. Am. Water Res. Assoc.*, **42**, 901–914.
- Kingsford, M. J., Leis, J. M., Shanks, A. *et al.* (2002) Sensory environments, larval abilities and local self-recruitment. *Bull. Mar. Sci.*, **70**, 309–340.
- Levin, L. A. (1986) The influence of tides on larval availability in shallow waters overlying a mudflat. *Bull. Mar. Sci.*, **39**, 224–233.
- Liu, W. C. (2005) Modeling the influence of settling velocity on cohesive sediment transport in Tanshui River estuary. *Environ. Geol.*, **47**, 535–546.
- Liu, W. C., Hsu, M. H. and Kuo, A. Y. (2002) Modeling of hydrodynamics and cohesive sediment transport in Tanshui River estuarine system, Taiwan. *Mar. Pollut. Bull.*, **44**, 1076–1088.
- Mariani, S., Uriz, M.-J., Turon, X. *et al.* (2006) Dispersal strategies in sponge larvae: integrating the life history of larvae and the hydrologic component. *Oecologia*, **149**, 174–184.
- Miller, C. B. (1983) The zooplankton of estuaries. In Ketchum, B. K. (ed.), *Estuaries and Enclosed Seas*. Elsevier Scientific Publishing Company, Amsterdam, Netherlands, pp. 103–149.
- Miller, C. B. and Judkins, D. C. (1981) Design of pumping systems for sampling zooplankton, with descriptions of two high-capacity sampler for coastal studies. *Biol. Oceanogr.*, **1**, 29–56.
- Pawlik, J. R., Butman, C. A. and Starczak, V. R. (1991) Hydrodynamic facilitation of gregarious settlement of a reef-building tube worm. *Science*, **251**, 421–424.
- Peterson, P. and Stromberg, A. J. (1998) A simple test for departures from multivariate normality. *Department of Statistics Technical Report 373*. University of Kentucky, Lexington, KY.
- Pernet, B., Qian, P.-Y., Rouse, G. *et al.* (2002) Phylum Annelida. In Young, C. M., Sewell, M. A. and Rice, M. E. (eds), *Atlas of Marine Invertebrate Larvae*. Academic Press, San Diego, CA, pp. 209–243.
- Queiroga, H. and Blanton, J. (2004) Interactions between behaviour and physical forcing in the control of horizontal transport of decapod crustacean larvae. *Adv. Mar. Biol.*, **47**, 107–214.
- Rencher, A. C. (1995) *Methods of Multivariate Analysis*. J. Wiley, New York.
- SAS Institute. (2003) *SAS User's Guide: Statistics, Release 9.1*. SAS Institute, Cary, NC.
- Seuront, L., Schmitt, F. G., Brewer, M. C. *et al.* (2004) From random walk to multifractal random walk in zooplankton swimming behavior. *Zool. Stud.*, **43**, 498–510.
- Shanks, A. L. (1995) Mechanisms of cross-shelf dispersal of larval invertebrate and fish. In McEdward, L. (ed.), *Ecology of Marine Invertebrate Larvae*. CRC Press, Boca Raton, FL, pp. 323–368.

- Shanks, A. L., Largier, J., Brink, L. *et al.* (2002) Observations on the distribution of meroplankton during a downwelling event and associated intrusion of the Chesapeake Bay estuarine plume. *J. Plankton Res.*, **24**, 319–416.
- Shanks, A. L., Largier, J. and Brubaker, J. (2003) Observations on the distribution of meroplankton during an upwelling event. *J. Plankton Res.*, **25**, 645–667.
- Sulkin, S. D. (1984) Behavioral basis of depth regulation in the larvae of brachyuran crabs. *Mar. Ecol. Prog. Ser.*, **15**, 181–205.
- Wooldridge, T. and Erasmus, T. (1980) Utilization of tidal currents by estuarine zooplankton. *Estuarine Coastal Mar. Sci.*, **11**, 107–114.
- Wu, J. T. (1999) A generic index of diatom assemblages as bioindicator of pollution in the Keelung River of Taiwan. *Hydrobiologia*, **397**, 79–87.
- Yu, Y. (2005) Seasonal distribution of copepods in relation to environmental factors in Tanshui and Kaoping estuaries. Master Degree Thesis. Department of Marine Biotechnology and Resources, National Sun Yat Sen University, Kaohsiung, Taiwan (in Chinese).